Characterization of Stable Beryllium Fluoride, Aluminum Fluoride, and Vanadate Containing Myosin Subfragment 1–Nucleotide Complexes†

Moshe M. Werber,‡ Y. Michael Peyser,§ and Andras Muhlrad*,§

Department of Oral Biology, The Hebrew University-Hadassah School of Dental Medicine, Jerusalem 91010, Israel, and Bio-Technology General, Kiryat Weizmann, Rehovot 76236, Israel

Received March 6, 1992

ABSTRACT: Beryllium and aluminum fluorides are good phosphate analogues. These compounds, like orthovanadate, form stable complexes with myosin subfragment 1 (S1) in the presence of MgADP. The formation of the stable S1–nucleotide complexes is characterized by the loss of ATPase activity. For the complete loss of ATPase activity there was necessary a higher concentration of aluminum than of beryllium or vanadate. In the presence of MgATP the onset of the inhibition is delayed, which indicates that stable complexes cannot form when a specific site is occupied by the γ-phosphate of ATP or by P_i derived from the γ-phosphate. The half-lives of the S1–MgADP–(BeF_3^-), S1–MgADP–(AlF_4^-), and S1–MgADP–Vi complexes at 0 °C are 7, 2, and 4 days, respectively. In the presence of actin the rate of decomposition of all of the complexes is significantly enhanced; however, the order of decomposition is reversed, the fastest rate being observed with beryllium and the slowest with aluminum. The formation of the S1–MgADP–(BeF_3^-) and S1–MgADP–(AlF_4^-) complexes is accompanied by an increase in tryptophan fluorescence similar to that observed upon addition of MgATP to S1. The fluorescence increase develops rather slowly, by suggesting that the rate-limiting step in the formation of the stable complex is an isomerization. The rate of the fluorescence change accompanying the formation of the Be complex is faster than that for the Al complex. Addition of vanadate to S1 causes a static quenching of the tryptophan fluorescence. When ADP was added to S1–vanadate, there was a fast transient fluorescence increase followed by a slow decrease. The transient increase probably accompanies the appearance of the S1–MgADP complex, while the decrease is indicative of the formation of the stable S1–MgADP–Vi complex. The activation energy for the formation of the complexes, which was estimated from the temperature dependence of the fluorescence change, is about twice as high for the Al complex as for the other two stable complexes. The rate of formation of the Be and vanadate complexes displays a hyperbolic dependence on Be^{2+} and vanadate concentration, respectively, while the concentration dependence of the formation of the Al complex is rather complicated and has at least two components. The Be- and Al–S1 complexes, as opposed to uncomplexed S1, are not cleaved by vanadate-induced photocleavage at sites which are located at or in the proximity of the "consensus" ATP-binding site of myosin, viz., at 23 and 31 kDa from the N terminus. The results indicate that the three stable complexes are good analogues of the M**–MgADP–P_i transition state of the myosin-catalyzed ATP hydrolysis, and their study can help to elucidate the mechanism of the process.

The direct source of energy, required for muscle contraction and for a number of events in cell motility, derives from myosin-catalyzed ATP hydrolysis. The ATP-binding site of myosin resides on the "head" segment of the molecule, called S1.[1] ATP hydrolysis takes place in a sequence of events. During the various stages of the process a number of discrete intermediates is formed; these are all S1–nucleotide complexes. The structure of these intermediates is of great importance in studying the active site structure and the mechanism of myosin-catalyzed ATP hydrolysis. The predominant intermediate of the ATP hydrolysis is the M**–MgADP–P_i complex (Trentham et al., 1976). [M is the symbol for the myosin head, and the asterisks imply conformational changes manifesting themselves by a fluorescence increment (Werber et al., 1972).] This complex has a special significance in the molecular mechanism of muscle contraction, since its decomposition is believed to be directly responsible for the power stroke in the mechanical cross-bridge cycle (Taylor, 1979). The M**–MgADP–P_i transition state is relatively stable, having a half-life of several seconds at 25 °C (Trentham et al., 1976). However, to perform a detailed structural analysis of the complex, further stabilization of the transition state by nucleotide or phosphate analogues is indispensable.

Vanadate, which is a good structural analogue of phosphate (Lindquist et al., 1973), is known to stabilize transition states of various phosphotransferases and nucleotidases by substituting for phosphate. Vanadate exists in various forms, and the structure of orthovanadate closely resembles that of phosphate, with the distance of the V–O bond of 0.3 Å being longer than that of the P–O bond (Pope & Dale, 1968). It has been shown that vanadate readily forms a stable complex with myosin in the presence of Mg and ADP and that the M–MgADP–Vi complex, which contains MgADP and Vi in a "trapped" form, is in many respects similar to the M**–MgADP–P_i transition state of the myosin-catalyzed ATP hydrolysis (Goodno, 1979; Goodno & Taylor, 1982; Smith & Eisenberg, 1990). Substituting photoaffinity analogues of ADP for ADP in the stable M–MgADP–Vi complex has proved useful in locating the nucleotide-binding site on S1 (Cole & Yount, 1990). The use of vanadate also helped in

† This research was supported by Grant 88-00018 from the United States–Israel Binational Research Foundation (BSF), Jerusalem, Israel.

* Author to whom correspondence should be addressed.

‡ Bio-Technology General.

§ The Hebrew University.

[1] Abbreviations: S1, myosin subfragment 1; Vi, vanadate; DTE, dithioerythritol; SDS–PAGE, sodium dodecyl sulfate–polyacrylamide gel electrophoresis.

0006-2960/92/0431-7190$03.00/0

detecting the phosphate-binding site of S1. Irradiation by near-UV light in the presence of vanadate cleaves the S1 heavy chain at sites located 23, 31, and 74 kDa from the N terminus, and it has been assumed that these cleavage sites indicate the location of the phosphate-binding sites (Grammer et al., 1988; Mocz, 1989; Ringel et al., 1990).

It has been recently shown that beryllium and aluminum fluoride complexes (BeF_3^- and AlF_4^-) are also good structural analogues of inorganic orthophosphate (Chabre, 1990). Different complexes of aluminum or beryllium fluoride are spontaneously formed in the presence of aluminum or beryllium and fluoride ions (Goldstein, 1964; Martin, 1988). The distances of the Be–F and Al–F bonds are identical to that of the P–O bond, i.e. 1.55 Å (Post & Kotz, 1975). Like vanadate, these phosphate analogues are only active in conjunction with a bound nucleotide diphosphate and can stabilize enzyme–nucleotide complexes (Chabre, 1990), including those of actin (Combeau & Carlier, 1989, 1990), smooth muscle heavy meromyosin (Maruta et al., 1991), and skeletal myosin S1 (Phan & Reisler, 1992; Beck et al., 1992). However, in spite of the similarity in their stabilizing effect of these complexes, the structures of beryllium and of the analogous aluminum fluoride are different from that of orthovanadate. Vanadate readily forms a pentavalent bipyramidal structure (Lindquist et al., 1973), like that of γ-phosphate in ATP undergoing hydrolysis: it therefore stabilizes a structure analogous to that of the transition state. In contrast to the configuration of vanadate, beryllium bonding to the fluoride atoms is strictly tetrahedral (Chabre, 1990), and therefore, it mimics the γ-phosphate in ATP prior to the hydrolysis or the bound orthophosphate following the hydrolysis. (The similarities in the binding properties of AlF_4^- and BeF_3^- complexes suggest, but do not prove, that the aluminum complex also has a tetrahedral geometry.) It follows from the foregoing that S1-MgADP-Vi and S1-MgADP-(BeF_3^-) may represent different intermediates of the ATP cycle. S1–MgADP–Vi is probably analogous to the transition state of the M*–MgATP $\rightleftharpoons$ M**–MgADP–P_i reaction, while S1–MgADP–(BeF_3^-) may mimic the M**–MgADP–P_i or the M*–MgATP species. Therefore, the study of the structure of various stable S1 complexes, formed by vanadate, BeF_3^-, or AlF_4^-, may reveal important structural changes, which take place in S1 during the ATP cycle. In light of the foregoing, we launched a comparative study of the formation, decomposition, and structure of the stable S1–MgADP complexes containing beryllium fluoride, aluminum fluoride, or vanadate using enzymatic, fluorescence, and photocleavage techniques. The results indicate that MgADP–(BeF_3^-) and MgADP–(AlF_4^-), similarly to MgADP–Vi, are trapped at the ATP-binding site of S1. The characteristics of the three stable complexes are similar to those of the M**–MgADP–P_i transition state. However, significant differences were found in the formation, decomposition, and stability of the stable complexes; these can be useful in elucidating the mechanism of myosin-catalyzed ATP hydrolysis. Preliminary reports of this work have been presented (Muhlrad & Peyser, 1991; Muhlrad et al., 1992).

MATERIALS AND METHODS

Reagents. ATP, ADP, DTE, Hepes, Tris, NaF, sodium orthovanadate, $BeCl_2$, $AlCl_3$, and chymotrypsin were of the Sigma best grade. All other chemicals were of reagent grade. A stock solution of sodium vanadate (100 mM) was prepared according to the method of Goodno (1979). Stock solution of $BeCl_2$[2] was 1% in 1% HCl, and it was neutralized before use by NaOH to pH 5.5.

Proteins. Myosin and actin were prepared from the back and leg muscles of rabbit, according to the methods of Tonomura et al. (1966) and Spudich and Watt (1971), respectively. S1, the head fragment of myosin, was prepared by digesting myosin filaments with chymotrypsin according to the procedure of Weeds and Taylor (1975). Protein concentrations were estimated from absorption, by assuming an A (1%) at 280 nm of 7.5 and an A (1%) at 290 nm of 6.4 for S1 and actin, respectively. Molecular masses of S1 and actin were assumed to be 115 and 42 kDa, respectively.

Preparation of Stable S1–Nucleotide Complexes (Trapping). Trapping by vanadate was performed essentially by the method of Goodno (1982). S1 (20–50 μM) was incubated for 5 min at 25 °C with 1 mM $MgCl_2$, 50 mM Tris-HCl, pH 7.9, and 0.2 mM ADP. After that time, 0.2 mM Vi was added and the incubation was continued for 15 min at 25 °C. In the case of $BeCl_2$ and $AlCl_3$, 20–50 μM S1 was incubated for 5 min at 25 °C in 1 mM $MgCl_2$, 50 mM Tris-HCl, pH 7.9, 0.2 mM ADP, and 5 mM NaF (this latter was prepared freshly in a plastic tube each day). After addition of 0.2 mM $BeCl_2$ or 0.2 mM $AlCl_3$, the reaction mixture was further incubated at 25 °C for 15 min. Following incubation, the samples were dialyzed against 30 mM Tris-HCl, pH 7.9, 1 mM $MgCl_2$, and 30 mM NaCl overnight or the samples were gel-filtered through an NAD-5 column (Pharmacia) containing Sephadex G-25.

ATPase Assay. Following the trapping and removal of the nonbound, excess reagents, ATPase assays were carried out on the samples at 25 °C in 1-mL aliquots containing 0.1–0.2 μM S1, 2 mM ATP, 600 mM KCl, 50 mM Tris-HCl, pH 7.9, and 6 mM EDTA for K^+ (EDTA)-activated ATPase or 6 mM $CaCl_2$ for Ca^{2+}-activated ATPase. Actin-activated S1 ATPase was measured at 25 °C in samples containing 0.1 μM S1, 0.5–1 μM F-actin, 1 mM ATP, 1 mM $MgCl_2$, and 30 mM HEPES, pH 7.0. Mg-modulated ATPase was assayed under the same conditions but in the absence of actin. ATPase activities (micromoles of P_i per milligram of S1 per minute) were calculated from production of inorganic phosphate (P_i) using the Fiske and Subbarow (1925) method. Incubation times were chosen so that less than 15% of the ATP was hydrolyzed, and thus initial rates were obtained.

Vanadate-Induced Photocleavage of S1. This was carried out on 8 μM S1 at 30 mM HEPES, pH 7.0, 1 mM $MgCl_2$, and 0.5 mM Vi on stable S1–MgADP–(BeF_3^-) or S1–MgADP–(AlF_4^-) complexes following the removal of excess reagent by gel filtration or by dialysis. The samples were irradiated by a UV transilluminator (U.V.P. Inc.) in ice, using near-ultraviolet light (peak 365 nm) for 10–30 min (Ringel et al., 1990).

SDS-PAGE. Electrophoretic analysis of the samples was carried out on 7–18% polyacrylamide gradient gels. The peptide bands were visualized by staining with Coomassie Brilliant Blue. Molecular masses of the peptide bands were estimated by comparing their mobilities with those of authentic markers.

Fluorescence Measurements. These measurements were performed in a Jasco FP-770 spectrofluorometer on 0.9–1 μM S1 in 1 mM $MgCl_2$, 30 mM Tris-HCl, pH 7.9, 0.2 mM ADP, and 5 mM NaF. Different concentrations of $BeCl_2$ (10–400 μM), $AlCl_3$ (10–800 μM), or sodium vanadate (10–200 μM) were also added. (In the case of vanadate NaF was

[2] Beryllium and its salts are extremely toxic, even at low concentrations; therefore, appropriate precautions should be taken in handling all of the beryllium-containing solutions.

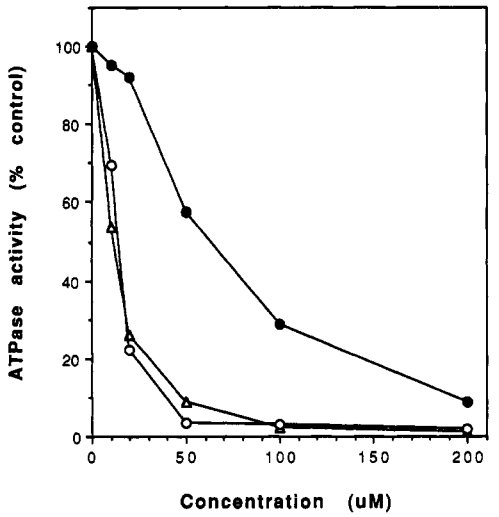

FIGURE 1: Dependence of the loss of ATPase activity upon concentration of $BeCl_2$, $AlCl_3$, or vanadate during formation of stable S1–nucleotide complexes. S1, 20 μM, was incubated at 25 °C for 15 min in 0.2 mM ADP, 1 mM $MgCl_2$, 30 mM Tris-HCl (50 mM Tris-HCl in the case of vanadate), pH 7.9, 5 mM NaF (in the case of $BeCl_2$ and $AlCl_3$), and $BeCl_2$, $AlCl_3$, or sodium vanadate as indicated on the abscissa. Following the incubation, aliquots were taken from the samples, and their K^+(EDTA)-activated ATPase activity was measured as described under Materials and Methods. ATPase activity was expressed as percent of control. (○) $BeCl_2$; (●) $AlCl_3$; (△) vanadate.

absent.) The measurements were carried out at constant temperature, ranging between 5 and 25 °C. The excitation wavelength selected was 295 nm, and the excitation and emission slits were both at 5 nm, so as to ensure that only tryptophans were excited (Werber et al., 1972). The emission was monitored in the range between 310 and 390 nm. When the kinetics of the formation of the fluorescent change was measured, the emission was monitored at 335.5 nm, which was the peak of the emission spectrum.

RESULTS

The formation of stable enzyme–substrate or enzyme–product complexes is accompanied by the loss of enzyme activity as was shown for the vanadate inhibition of ATPase by Goodno (1979) and for the aluminum fluoride inhibition of smooth muscle heavy meromyosin by Maruta et al. (1991). We found that a 15-min incubation of S1 at 25 °C in the presence of NaF, MgADP, $BeCl_2$, or $AlCl_3$ leads to the essentially complete inhibition of Mg^{2+}-, Ca^{2+}-, or K^+(EDTA)-activated ATPase activities, while no inhibition was observed when any of the constituents was omitted. The dependence of the K^+ (EDTA)–ATPase activity of S1 on the concentration of $BeCl_2$, $AlCl_3$, and vanadate in the incubation mixture is presented in Figure 1. Virtually complete loss of activity was observed when S1 was preincubated with 50 μM $BeCl_2$ or vanadate in the presence of MgADP, while in the case of $AlCl_3$ a concentration of 200 μM was necessary to obtain the same degree of inhibition. Essentially, the same concentration dependence of the inhibition was observed when the Ca^{2+}- or actin-activated S1 ATPase was measured (data not shown). The inhibition of the ATPase activity is indicative of the formation of inert stable complexes.

When MgATP instead of MgADP was added to the reaction mixture, the onset of the inhibition of the Mg^{2+}-activated ATPase activity of S1 was significantly delayed (Figure 2). This retarded onset of inhibition was observed in the presence of $BeCl_2$ plus NaF, $AlCl_3$ plus NaF, and Vi, while virtually

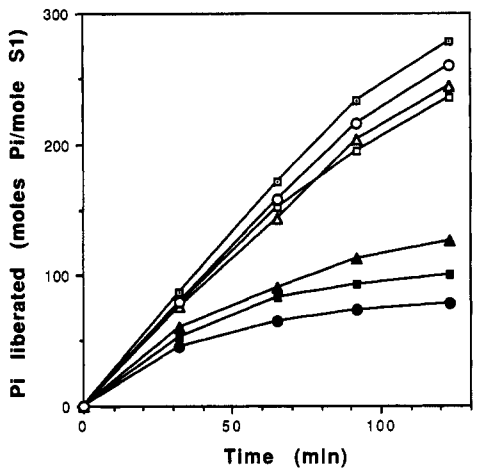

FIGURE 2: Effect of BeF_3^-, AlF_4^-, and vanadate on the Mg^{2+}-modulated ATPase activity of S1. ATP, 1 mM, was added to 0.5 μM S1 in 1 mM $MgCl_2$, 30 mM HEPES, pH 7.0, and 150 μM $BeCl_2$ (□], 150 μM $AlCl_3$ (△), 5 mM NaF (○), 150 μM $BeCl_2$ plus 5 mM NaF (■), 150 μM $AlCl_3$ plus 5 mM NaF (▲), 150 μM sodium vanadate (●), or no addition (⊡). The reaction mixture was incubated at 25 °C, and aliquots were taken for phosphate determination (see Materials and Methods) at the time intervals indicated on the abscissa.

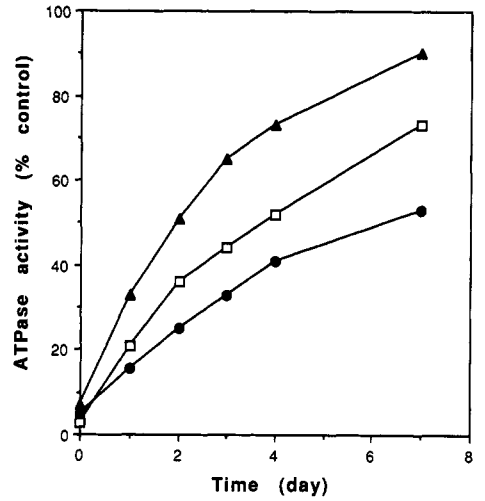

FIGURE 3: Recovery of ATPase activity upon incubation of stable S1–nucleotide complexes at 0 °C. Stable complexes were prepared as described under Materials and Methods. They were dialyzed against 1 mM $MgCl_2$, 30 mM NaCl, and 30 mM Tris-HCl, pH 7.9, at 0 °C to remove excess reagent for 1 day. Aliquots were taken for assaying K^+(EDTA)-activated ATPase before and several times after the dialysis as indicated on the abscissa. (●) BeF_3^-; (▲) AlF_4^-; (□) Vi.

no inhibition was noticed when either $BeCl_2$ or $AlCl_3$ without NaF or NaF without $BeCl_2$ or $AlCl_3$ was added. The order of the onset of the inhibition was Vi > $BeCl_2$ plus NaF > $AlCl_3$ plus NaF. These results indicate that no stable complex can be formed when the active site of myosin is occupied by either MgATP or MgADP plus P_i and that the phosphate analogues (Vi, BeF_3^-, or AlF_4^-) compete with phosphate for the same position in the active site.

After incubation of S1 with MgADP and either of the three phosphate analogues, the nonbound, excess reagent was removed from the solution by gel filtration or by dialysis. Only a few percent of the S1 ATPase activity was recovered after removal of the reagents (Figure 3). The highest recovery was observed with AlF_4^- and the smallest with BeF_3^-. The K^+ (EDTA)-activated S1 ATPase was monitored for several days after removal of the reagents. The recovery of the activity, which indicates the decomposition of the stable complexes, was rather slow. The half-lives of the stable complexes at 0

Table I: Rate Constants of Formation and Decomposition of S1–MgADP–(BeF_3^-), S1–MgADP–(AlF_4^-), and S1–MgADP–Vi Complexes[a]

constants	S1–MgADP–(BeF_3^-)	S1–MgADP–(AlF_4^-)	S1–MgADP–Vi
decomposition at 0 °C,[b] k_{-2} (s^{-1})	1.1×10^{-6}	4×10^{-6}	2×10^{-6}
half-life, $t_{1/2}$, of the complex at 0 °C[b] (days)	7	2	4
actin-induced decomposition at 25 °C,[c] k_{-2} (s^{-1})	$>2.8 \times 10^{-3}$	0.11×10^{-3}	0.95×10^{-3}
dissociation constant of the nonstable intermediate at 20 °C,[d] K_M (μM^{-1})	140	94[e]	50
complex formation at 20 °C,[d] k_2 (s^{-1})	14.3×10^{-2}	3.4×10^{-2} [e]	6.7×10^{-2}

[a] The reaction between BeF_3^-, AlF_4^-, and Vi (PA), on one hand, and S1–MgADP, on the other hand, is treated in analogy to the reaction of an enzyme with a substrate. By plotting $1/V$ against $1/[PA]$, two steady-state constants, $K_M = (k_2 + k_{-1})/k_1$ and $V_{max} = k_2[S1–MgADP–PA]$, can be obtained (see Scheme I). For the three phosphate analogues k_{-2}, which is the rate constant of the decomposition of the stable complex, is extremely small and, therefore, negligible, and k_2, the rate constant of the slow isomerization step, is assumed to be much smaller than k_{-1}. Therefore, K_M is equal to the dissociation constant of the nonstable intermediate, S1–MgADP–PA, and controls the rapid equilibrium mentioned in the text (Scheme I). [b] From Figure 3. [c] From Figure 4. [d] Estimated from the concentration dependence of rate of formation of stable complexes (Figure 9). The intercepts on the abscissa and on the ordinate are equal to $-1/K_M$ and $1/k_2$, respectively. [e] In the 20–500 μM Al^{3+} concentration range.

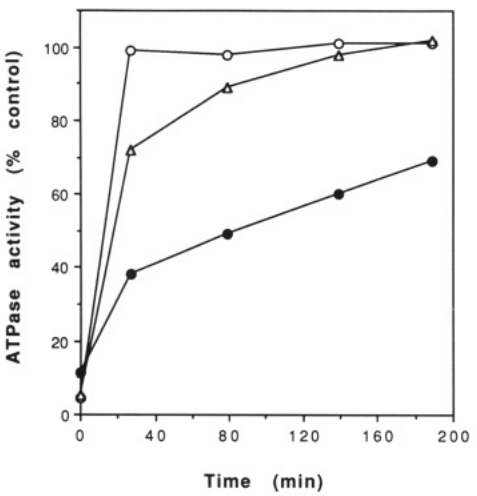

FIGURE 4: Actin-induced recovery of the ATPase activity of the stable S1–nucleotide complexes. Stable complexes were prepared, and the excess of reagents was removed by dialysis as described under Materials and Methods. F-actin, 10 μM, was added to 5 μM stable S1 complex in 50 mM KCl, 1 mM $MgCl_2$, and 30 mM Tris-HCl, pH 7.9, and was incubated at 25 °C. Aliquots were taken for assaying K^+ (EDTA)-activated ATPase activity at the time intervals indicated on the abscissa. ATPase activity was expressed as percent of uncomplexed S1 control. (○) S1–MgADP–(BeF_3^-); (●) S1–MgADP–(AlF_4^-); (△) S1–MgADP–Vi.

°C, estimated from the recovery rates, are 7 days for the beryllium-, 4 days for the vanadate-, and 2 days for the aluminum-containing S1 complex, respectively (Table I). Addition of actin dramatically accelerates the rate of decomposition of the stable complexes (Figure 4). In the presence of actin the half-life of the beryllium-containing S1 complex is much shorter than that of the aluminum complex, just the opposite of what is observed in the absence of actin. The effect of actin on the decomposition of the stable complexes is ionic strength dependent; it increases with decreasing ionic strength (results not shown).

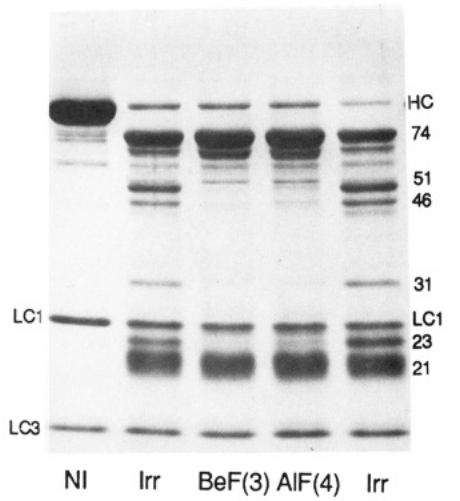

FIGURE 5: Vanadate-induced photocleavage of BeF_3^- and AlF_4^- containing stable S1–nucleotide complexes. Stable complexes were prepared, and the excess of reagents was removed by dialysis as described under Materials and Methods. To 8 μM S1 in 1 mM $MgCl_2$ and 30 mM HEPES, pH 7.0 was added 0.5 mM sodium vanadate; the mixture was irradiated by near-UV light in ice for 9 min and analyzed by SDS–PAGE (for details, see Materials and Methods). (NI) Non-irradiated S1; (Irr) irradiated and uncomplexed S1; [BeF(3)] S1–MgADP–(BeF_3^-); [AlF(4)] S1–MgADP–(AlF_4^-). Vertical numbers are molecular masses in kilodaltons. (HC) Heavy chain of S1; (LC1 and LC3) light chains of S1.

We have recently shown that irradiation with near-UV light cleaves the S1 heavy chain at three specific sites, viz., at 23, 31, and 74 kDa from the N terminus (Ringel et al., 1990; Muhlrad et al., 1991a). When the S1-MgADP–(BeF_3^-) or the S1–MgADP–(AlF_4^-) complex was irradiated by near-UV light in the presence of vanadate, only the 74-kDa cleavage was observed which is manifested in the appearance of the 74- and 21-kDa bands (Figure 5). It is assumed that an essential requirement for the photocleavage at the 23- and 31-kDa sites is the binding of Vi to the consensus binding site. Therefore, the lack of cleavage at these sites indicate that Vi cannot bind to the consensus ATP-binding site because it is already occupied by BeF_3^- or AlF_4^-. This means that BeF_3^- and AlF_3^- bind to the same site as Vi in the consensus ATP-binding site of myosin.

Preliminary results (Muhlrad & Peyser, 1991; Muhlrad et al., 1992) showed that the formation of S1–MgADP–(BeF_3^-) or S1–MgADP–(AlF_4^-) complexes was accompanied by an increase in the tryptophan fluorescence of S1, similar in magnitude to that described for the S1–MgADP–P_i complex (Werber et al., 1972). The formation of these complexes was found to be time-dependent, and the rate of development of the fluorescence increment was also dependent on the concentration of the phosphate analogue. In this work we studied in detail the dependence of the formation of both the S1–MgADP–(BeF_3^-) and S1-MgADP–(AlF_4^-) complexes, as well as that of S1–MgADP–Vi, both on the phosphate analogue concentration and on the temperature. Both the increment (or decrement) in fluorescence and the kinetics of its development were measured under the various conditions indicated.

The fluorescence emission spectra of S1, S1–MgADP, and S1–MgADP–(BeF_3^-) are shown in Figure 6A. The addition of 10–200 μM $BeCl_2$ to S1–MgADP in the presence of NaF in the temperature range 20–25 °C (see also below) causes a 9.4% (average) enhancement of the fluorescence intensity. Figure 6B shows the time course of the development of the

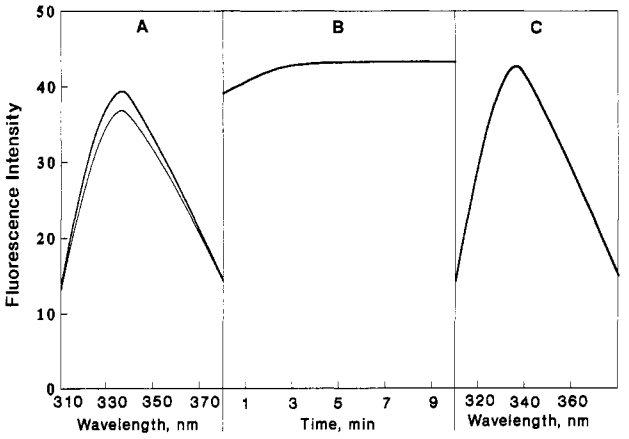

FIGURE 6: Fluorescence emission spectrum and kinetics of formation of the S1–MgADP–(BeF_3^-) complex. Excitation wavelength was 295 nm. All measurements were performed at 20 °C. (A) (lower curve) Emission spectrum of 0.9 μM S1 in 1 mM $MgCl_2$ and 30 mM Tris-HCl, pH 7.9; (upper curve) emission spectrum of the same S1 solution after addition of 0.2 mM ADP and 5 mM NaF. (B) Time course of the development of the fluorescent intensity increment at 335.5 nm following addition of 20 μM $BeCl_2$. (C) Emission spectrum of 0.9 μM S1–MgADP–(BeF_3^-) 20 min after addition of $BeCl_2$.

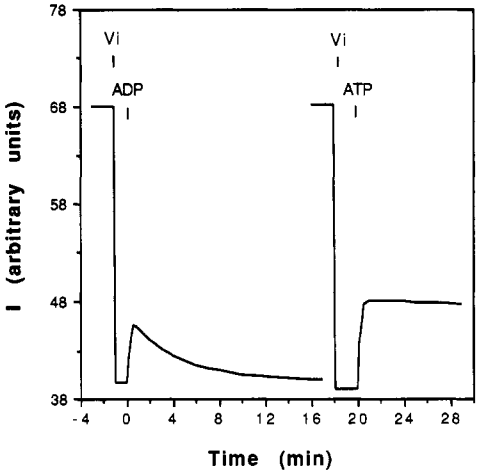

FIGURE 7: Fluorescence intensity changes accompany the formation of the S1–MgADP–Vi complex. Sodium vanadate, 0.2 mM, was added to 0.9 μM S1 in 1 mM $MgCl_2$ and 30 mM Tris-HCl, pH 7.9. This was followed by addition of 0.2 mM ADP or 0.2 mM ATP, and the fluorescence emission at 335.5 nm was recorded. Additions of reagents are indicated. Excitation wavelength was 295 nm. Measurements were performed at 20 °C. (Abscissa) Fluorescence intensity (I).

fluorescence increment with 20 μM $BeCl_2$ at 20 °C. The final spectrum achieved for S1–MgADP–(BeF_3^-) (20 min after the addition of $BeCl_2$) is shown in Figure 6C. Similar behavior follows the addition of various concentrations (between 10 and 800 μM) of $AlCl_3$ to S1–MgADP but with two differences: the magnitude of the fluorescence increment is larger (13.9%), and the kinetics of this development is slower (see below). On the other hand, the formation of the S1–MgADP–Vi complex is accompanied by a time-dependent *decrease* in fluorescence. Because vanadate causes a quenching of the fluorescence of S1, the kinetics was followed in this case by monitoring the decrease in fluorescence, subsequent to the addition of ADP to the S1-vanadate complex (Figure 7). Upon addition of ADP, first a transient fluorescence intensity increase is observed, which is followed by a decrease due to the formation of the stable S1–MgADP–Vi complex. However, when ATP was substituted for ADP, this latter time-dependent decrease was almost completely abolished. We studied the quenching of both S1 and the model compound

Table II: Normalized Increments or Decrements of Fluorescence Intensity Induced by Various Metal Ions Added to S1–MgADP[a]

metal ion	temp (°C)	concn (μM)	$\Delta F/F_0$[b] (%)
Al^{3+}	20	20–800	13.5
	5–25	800	14.5
Be^{2+}	20	10–200	9.8
	5	50	4.6
	10	50	4.1
	15	50	7.8
	20	50	9.4
	25	50	9.3
Vi[c]	20	10–200	−12.74
	7.5	50	−6.8
	10	50	−9.9
	15	50	−11.2
	20	50	−12.1
	25	50	−14.2

[a] Excitation 295 nm, emission 335.5 nm. For fluorescence measurements see Materials and Methods. [b] $\Delta F/F_0$, fluorescence intensity increment induced by the metal ions per fluorescence intensity of S1–MgADP before addition of metal ions. [c] In this case Vi was added first before ADP. F_0 is the maximal fluorescence intensity observed immediately after addition of ADP; ΔF is the decrement in intensity after the plateau at the end of the measurement is reached.

N-acetyltryptophanamide by vanadate in the concentration range 0–300 μM and found in both cases (after correction for inner filter effects) that the Stern–Volmer plot displays a strong upward curvature (data not shown). This means that the addition of vanadate causes a static type of quenching of the tryptophan fluorescence (Eftink & Ghiron, 1976).

In the case of AlF_4^-, approximately the same increment in fluorescence intensity was observed at the various temperatures between 5 and 25 °C, whereas in the cases of BeF_3^- and Vi the increment—or decrement—observed was temperature dependent; decreases in fluorescence changes were seen with the decreasing temperature. However, note that, as expected, because of the effect of temperature on fluorescence, the initial fluorescence of the S1–MgADP complex was higher at 15 °C (and other lower temperatures) than at 25 °C. The final changes in fluorescence, ΔF, increment (with Be^{2+} or Al^{3+}), or decrement in the case of vanadate, normalized with respect to the fluorescence intensity, F_0, of S1–MgADP, i.e., $\Delta F/F_0$ values, are summarized in Table II.

The time courses of the fluorescence change were fitted to a single exponential and characterized by a first-order kinetic constant (k_f) in all cases. The temperature dependence (5–25 °C) of the k_f values for the BeF_3^-, AlF_4^-, and vanadate complexes with S1–MgADP was analyzed by Arrhenius plots (Figure 8). Linear plots were obtained in all three cases, with the following energies of activation: Be^{2+}, E_a = 18.1 kcal/mol; Al^{3+}, measured at both saturation levels, at 300 μM E_a = 32.2 kcal/mol and at 800 μM E_a 29.2 kcal/mol; and Vi, E_a = 14.7 kcal/mol.

The dependence of the first-order kinetic constants (k_f) for the development of the fluorescence change (increment or decrement) at 20 °C on the concentration of the three phosphate analogues is shown in Figure 9. At high phosphate analogue concentrations k_f values approach saturation, which indicates that the formation of the stable complex is comprised of two steps: (i) a rapid binding equilibrium which is followed by (ii) a slow isomerization step according to

Scheme I

$$\text{M–MgADP} + \text{PA} \underset{k_{-1}}{\overset{k_1}{\rightleftharpoons}} \text{M–MgADP–PA} \underset{k_{-2}}{\overset{k_2}{\rightleftharpoons}} \text{M}^0\text{–MgADP–PA}$$

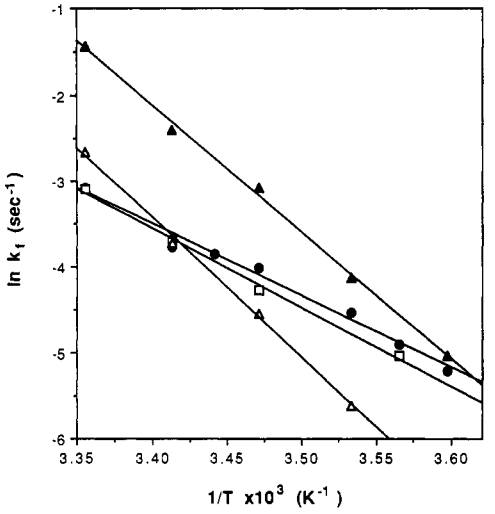

FIGURE 8: Temperature dependence (Arrhenius plot) of the rate of formation of the stable S1–nucleotide complexes. The rate constant of formation (k_f) was calculated from the time courses of the fluorescence change accompanying the formation of the stable complexes at various temperatures. For conditions of the fluorescence measurements, see Materials and Methods. Monitoring the fluorescence was started by addition of $BeCl_2$ and $AlCl_3$ or ADP in the case of vanadate. Metal ion concentrations: 50 μM Be^{2+} (●); 50 μM vanadate (□); 300 μM Al^{3+} (△); 800 μM Al^{3+} (▲).

where PA denotes phosphate analogue and M^0 indicates changed S1 conformation. A similar mechanism for vanadate binding has previously been proposed by Smith and Eisenberg (1990).

The dissociation constants of the rapid binding equilibrium, K_M, and the rate constants of the isomerization step, k_2, obtained by plotting the reciprocal value of k_f vs the reciprocal value of the phosphate analogue concentration, [PA], i.e., $1/k_f$ vs $1/[PA]$ (inset of Figure 9), are listed in Table I. The analysis of the kinetic parameters is developed under Table I.

DISCUSSION

The formation, decomposition, and structure of Vi, BeF_3^-, and AlF_4^- containing stable S1–nucleotide complexes were comparatively studied. The results show that S1 forms stable complexes with MgADP in the presence of all three phosphate analogues mentioned above. We assume that these complexes mimic the M**–MgADP–P_i transition state of the ATP hydrolysis for the following resons: (i) actin accelerates the decomposition of the complexes, and this actin-dependent decomposition is ionic strength dependent similarly as observed for the decomposition of the M**–MgADP–P_i transition state (Taylor, 1979); (ii) the formation of the complexes (except vanadate) is accompanied by an increase in S1 tryptophan fluorescence (Werber et al., 1972); and (iii) the vanadate-induced photocleavage of the stable complexes is inhibited at a site located 23 kDa from the N terminus, i.e., at the consensus ATP-binding site, in a manner similar to its inhibition in the presence of MgATP (Mocz, 1989; Muhlrad et al., 1991a), when 90% of S1 exists in the M**–MgADP–P_i form (Trentham et al., 1976). The finding that the onset of the inhibition of the ATPase activity by phosphate analogues is retarded in the presence of MgATP indicates that the stable complexes cannot form when the active site of S1 is occupied by either MgATP or MgADP plus P_i. This could be interpreted to mean that the P_i analogues occupy essentially the same position in the active site as that of the γ-phosphate of ATP before the hydrolysis or that of the P_i derived from

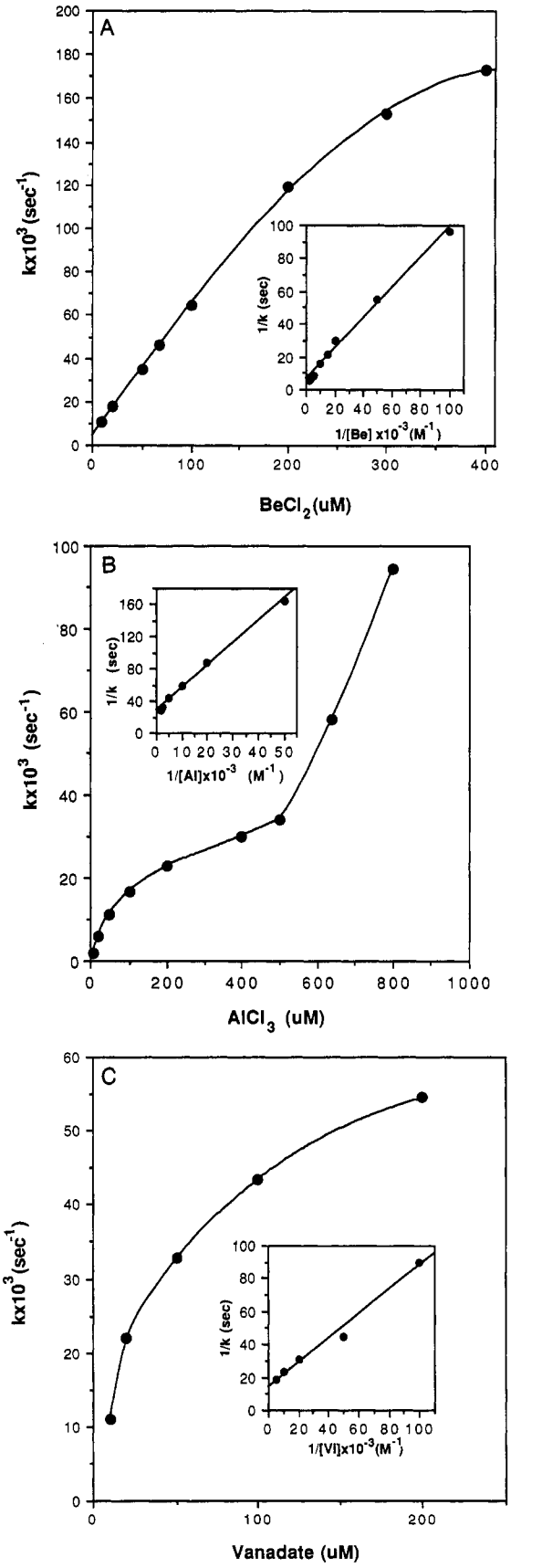

FIGURE 9: Dependence of the rate of formation of the stable S1–nucleotide complexes on the concentrations of $BeCl_2$, $AlCl_3$, and sodium vanadate. For conditions of the fluorescence measurements and calculation of the rate constants (k_f), see Figure 8 and Materials and Methods. Fluorescence measurements were performed at 20 °C. (Inset) Double-reciprocal plot ($1/k_f$ vs $1/mM$). (A) Beryllium; (B) aluminum, the inset contains only the 20–500 μM concentration range; (C) vanadate.

ATP after the hydrolysis. In conclusion, it can be assumed that the S1–MgADP–Vi, S1–MgADP–(BeF_3^-), and S1–MgADP–(AlF_4^-) complexes are good analogues of the M**–MgADP–P_i transition state.

The question arises whether the three stable complexes mimic the transient state of the ATP hydrolysis to the same degree or whether significant differences exist among them. The findings of the present study support the second possibility. Significant differences were found in the formation, in the stability, and in the actin-induced decomposition of the complexes. By studying the concentration dependence of the formation of the complexes, it was shown that a much smaller concentration of $BeCl_2$ was necessary for the formation of S1–MgADP–(BeF_3^-) as compared to the concentration of $AlCl_3$ required for the production of the S1–MgADP–(AlF_4^-), while the concentration of Vi necessary for the formation of the S1–MgADP–Vi complex was in between the two extremes. The stability of the BeF_3^--containing complexes was the highest, and that of the AlF_4^--containing complex was the lowest in the absence of actin. Addition of actin dramatically increases the rate of decomposition of the complexes and reverses the order of stability: in the presence of actin the stability of S1–MgADP–(AlF_4^-) is the highest and that of S1–MgADP–(BeF_3^-) is the lowest. From the point of view of the actin effect the S1–MgADP–(BeF_3^-) mimics best, and the Al complex mimics least, the M**–MgADP–P_i transition state, whose rate of decomposition is increased by actin by about the same factor (1000-fold) (Taylor, 1979) as that of the BeF_3^--containing complex. Differences were also found in the rates of formation of the complexes, which were estimated from the time course of the fluorescence change. The rate of the formation of the BeF_3^--containing complex was higher by an order of a magnitude than that of the AlF_4^--containing complex, while the middle position was again occupied by the Vi complex.

By studying the dependence of the rate of development of the fluorescence change on concentration and on temperature, valuable information could be obtained about the formation and structure of the stable complexes. The fact that the formation of the complexes is accompanied by a change in tryptophan fluorescence emission indicates that conformational changes are taking place in the S1 structure during the process. We assume that the conformational changes observed upon the formation of the AlF_4^-- and BeF_3^--containing complexes are similar to those which accompany the production of the M**–MgADP–P_i transition state, because similar fluorescence increments are observed in all of these processes. This situation exists at all of the temperatures employed in studying the formation of S1–MgADP–(AlF_4^-). However, in the case of BeF_3^-- and Vi-containing complexes the amplitude of the fluorescence increment—or decrement—is temperature dependent. In the range 15–25 °C the increment accompanying the formation of the Be complex is similar to that obtained upon forming the M**–MgADP–P_i transition state, while in the range 5–15 °C it is similar to that observed upon forming another, possibly the M*–MgATP intermediate. This finding indicates that at higher temperature the S1–MgADP–BeF_3^- complex mimics the former, while at lower temperatures the prevalent form of the complex is similar to the latter intermediate in myosin-catalyzed ATP hydrolysis. The Be and probably the Vi complex of S1 may exist as two conformers, and the equilibrium between the two conformers is temperature dependent as suggested by Shriver and Sykes (1981). The rate of the development of the fluorescence change accompanying the formation of the three stable complexes is rather slow, in comparison with the rates of simple protein–ligand association. This slowness was interpreted by Goodno (1979)—in the case of the vanadate complex—in terms of a rate-limiting isomerization step, which follows the binding of the ligands, MgADP and Vi, at the myosin ATPase site. Since the rate of the forming of the AlF_4^-- and BeF_3^--containing complexes is essentially of the same magnitude as that of forming the Vi complex, we assume that with all three phosphate analogues the fluorescence change reflects a rate-limiting isomerization step, at least at saturating concentrations. At lower phosphate analogue concentrations, the ligand–protein association steps become rate limiting, as reflected in the concentration dependence curves of the rate of development of the fluorescence change (Figure 9). For a fixed concentration of phosphate analogue, the kinetics are describable by pseudo-first-order rate constants. The phosphate analogue concentration dependence of the forming of the complexes, at least in the case of Vi and BeF_3^-, is of the quasi hyperbolic type. This hyperbolic dependence is characteristic of active-site-directed reagents, whose binding takes place prior to an isomerization reaction. The concentration dependence curve of the formation of the S1–MgADP–(AlF_4^-) complex is rather special: it is made up of two distinctive phases (Figure 9B). The simplest interpretation of the two-phase curve is that there exist on S1 two sites, which bind AlF_4^- and which are involved in the regulation of the formation of the S1–MgADP–(AlF_4^-) complex. The first is a high-affinity site, which is presumably part of the ATP-binding site; there exists, however, a second, low-affinity site, whose occupation by AlF_4^- accelerates the rate of the fluorescence change but does not affect the magnitude of the fluorescence increment. There is also another possibility, i.e., that the two-phase curve is the result of the concentration-dependent distribution of the multiple aluminum fluoride ionic species present in the solution.

For both S1 and a model compound, *N*-acetyltryptophanamide, a static type of quenching was observed upon addition of vanadate. This indicates that, unexpectedly, all S1 tryptophans are accessible to vanadate. Addition of ADP to S1 in the presence of Mg and vanadate causes a fast transient increase in fluorescence intensity. We assume that the fluorescence intensity increase is due to the formation of the M*–MgADP complex, which then reacts with vanadate and finally is transformed in the slow isomerization step to the quenched stable S1–MgADP–Vi complex. This isomerization step is accompanied by a decrease in fluorescence intensity, which is probably caused by fluorescence resonance energy transfer taking place between the vanadate incorporated into S1 and a nearby tryptophan (or tryptophans) in the protein structure. This decrease in fluorescence intensity is prevented when ATP is used instead of ADP (Figure 7), since in this case the vanadate cannot occupy the position of the γ-phosphate of ATP (see above). According to this hypothesis the formation of the stable vanadate-containing complex takes place according to

Scheme II

$$\mathrm{M} + \mathrm{MgADP} \underset{k_{-1}}{\overset{k_1}{\rightleftarrows}} \mathrm{M^*{-}MgADP} + \mathrm{Vi} \underset{k_{-2}}{\overset{k_2}{\rightleftarrows}} \mathrm{M^*{-}MgADP{-}Vi} \underset{k_{-3}}{\overset{k_3}{\rightleftarrows}} \mathrm{M^0{-}MgADP{-}Vi}$$

The rate constant, k_2, depends on the vanadate concentration, whereas k_3 is the rate constant governing the formation of the final stable complex. M* and M^0 denote conformational

changes in S1 structure which are manifested as altered fluorescence intensity.

Near-UV irradiation in the presence of vanadate has been shown to cleave S1 heavy chain at sites located 23 and 74 kDa from the N terminus (Grammer et al., 1988; Mocz, 1989). The 23-kDa cleavage site was located at Ser-180 (Cremo et al., 1989), which is part of the consensus ATP-binding site of myosin (Walker et al., 1982). We have recently found an additional photocleavage site at 31 kDa from the N terminus of the S1 heavy chain (Ringel et al., 1990; Muhlrad et al., 1991a). The vanadate-induced photocleavage is specifically inhibited at the 23- and 31-kDa sites by ATP and by sulfate and at the 74-kDa site by actin (Muhlrad et al., 1991a,b). On the basis of these results, we assumed that the regulation of the cleavage at both the 23- and 31-kDa sites is linked and distinct from the regulation at the 74-kDa site. Our present findings that, in the stable S1–MgADP–(BeF_3^-) and S1–MgADP–(AlF_4^-) complexes, the vanadate-induced photocleavage is inhibited at both the 23- and 31-kDa sites and only the 74-kDa cut takes place is in agreement with the above conclusion. According to the 3D S1 model of Botts et al. (1989) the 23- and 31-kDa cleavage sites might be proximal to each other through a loop in the tertiary structure. This assumption is further supported by the results of Grammer and Yount (1991), which have shown that Ser-243, which is proximal to the 31-kDa site (Muhlrad et al., 1991a), is also proximal to the consensus ATP-binding site, or, in other words, to the 23-kDa cleavage site.

In conclusion, it has been found that the stable S1–MgADP–(BeF_3^-) and S1–MgADP–(AlF_4^-) complexes are, like S1–MgADP–Vi, good analogues of the M**–MgADP–P_i transition state of the myosin-catalyzed ATP hydrolysis. Along with basic similarity, there are significant differences between the stable complexes, suggesting that they mimic different stages of the transition process. In the future, these differences can be exploited in a more detailed study of the location and the tertiary structure of the ATP-binding site of myosin and the conformational changes taking place in myosin structure during the ATP hydrolysis.

REFERENCES

Beck, T. W., Chase, P. B., & Kushmerick, M. J. (1992) *Biophys. J. 61*, 2506a.

Botts, J., Thomason, J. F., & Morales, M. F. (1989) *Proc. Natl. Acad. Sci. U.S.A. 86*, 2204–2208.

Chabre, M. (1990) *Trends Biochem. Sci. 15*, 6–10.

Cole, D. G., & Yount, R. G. (1990) *J. Biol. Chem. 265*, 22537–22546.

Combeau, C., & Carlier, M.-F. (1989) *J. Biol. Chem. 264*, 19017–19021.

Combeau, C., & Carlier, M.-F. (1990) *J. Biol. Chem. 265*, 17429–17436.

Corbridge, D. E. C. (1974) *The Structural Chemistry of Phosphorous*, Elsevier, Amsterdam.

Cremo, C. R., Grammer, J. C., & Yount, R. G. (1989) *J. Biol. Chem. 264*, 6608–6611.

Eftink, M. R., & Ghiron, C. A. (1976) *Biochemistry 15*, 672–680.

Fiske, C. H., & Subbarow, Y. (1925) *J. Biol. Chem. 66*, 375–400.

Goldstein, G. (1964) *Anal. Chem. 36*, 243–244.

Goodno, C. C. (1979) *Proc. Natl. Acad. Sci. U.S.A. 76*, 2620–2624.

Goodno, C. C. (1982) *Methods Enzymol. 85*, 116–122.

Goodno, C. C., & Taylor, E. W. (1982) *Proc. Natl. Acad. Sci. U.S.A. 79*, 21–25.

Grammer, J. C., & Yount, R. G. (1991) *Biophys. J. 59*, 226a.

Grammer, J. C., Cremo, C. R., & Yount, R. G. (1988) *Biochemistry 27*, 8408–8415.

Lindquist, R. N., Lymn, J. L., & Lienhard, G. E. (1973) *J. Am. Chem. Soc. 95*, 8762–8768.

Martin, R. B. (1988) *Biochem. Biophys. Res. Commun. 155*, 1194–1200.

Maruta, S., Henry, G. D., Sykes, B. D., & Ikebe, M. (1991) *Biophys. J. 59*, 436a.

Mocz, G. (1989) *Eur. J. Biochem. 179*, 373–378.

Muhlrad, A., & Peyser, Y. M. (1991) *J. Muscle Res. Cell Motil. 13*, 246.

Muhlrad, A., Peyser, Y. M., & Ringel, I. (1991a) *Biochemistry 30*, 958–965.

Muhlrad, A., Peyser, Y. M., & Ringel, I. (1991b) *Eur. J. Biochem. 201*, 409–415.

Muhlrad, A., Peyser, Y. M., & Werber, M. M. (1992) *Biophys. J. 61*, 148a.

Phan, B. C., & Reisler, E. (1992) *Biophys. J. 61*, 1721a.

Pope, M. T., & Dale, D. W. (1968) *Q. Rev., Chem. Soc. 22*, 527–548.

Post, E. W., & Kotz, J. C. (1975) in *Inorganic Chemistry Series II* (Emeleus, H. J., Ed.), Vol. 1, pp 220–248, Butterworth, London.

Ringel, I., Peyser, Y. M., & Muhlrad, A. (1990) *Biochemistry 29*, 9091–9096.

Saraste, M., Sibbald, P. R., & Wittinghofer, A. (1990) *Trends Biochem. Sci. 15*, 430–434.

Shriver, J. W., & Sykes, B. D. (1981) *Biochemistry 20*, 2004–2012.

Smith, S. J., & Eisenberg, E. (1990) *Eur. J. Biochem. 193*, 69–73.

Spudich, J. A., & Watt, S. (1971) *J. Biol. Chem. 246*, 4866–4871.

Taylor, E. W. (1979) *CRC Crit. Rev. Biochem. 6*, 103–114.

Tonomura, Y., Appel, P., & Morales, M. F. (1966) *Biochemistry 5*, 515–521.

Trentham, D. R., Eccleston, J. F., & Bagshaw, C. R. (1976) *Q. Rev. Biophys. 9*, 217–281.

Walker, J. E., Saraste, M., Runswich, M. J., & Gay, N. J. (1982) *EMBO J. 1*, 945–951.

Weeds, A. G., & Taylor, R. S. (1975) *Nature (London) 257*, 54–56.

Werber, M. M., Szent-Gyorgyi, A. G., & Fasman, G. D. (1972) *Biochemistry 11*, 2872–2883.